Check for updates

Received: 29 July 2022 | Revised: 15 September 2023 | Accepted: 18 September 2023

DOI: 10.1002/nbm.5060

RESEARCH ARTICLE

NMR IN BIOMEDICINE WILEY

Implementation of pure shift ^{1}H NMR in metabolic phenotyping for structural information recovery of biofluid metabolites with complex spin systems

Jose Ivan Serrano-Contreras[1] | John C. Lindon[2] | Gary Frost[1] | Elaine Holmes[1,3,4] | Jeremy K. Nicholson[3,4,5] | Isabel Garcia-Perez[1]

[1]Department of Metabolism, Digestion and Reproduction, Division of Digestive Diseases, Section of Nutrition, Faculty of Medicine, Imperial College London, London, UK

[2]Department of Metabolism, Digestion and Reproduction, Division of Systems Medicine, Imperial College London, London, UK

[3]Australian National Phenome Centre, Computational and Systems Medicine, Health Futures Institute, Murdoch University, Perth, Western Australia, Australia

[4]Center for Computational and Systems Medicine, Health Futures Institute, Murdoch University, Perth, Western Australia, Australia

[5]Imperial College London, Institute of Global Health Innovation, London, UK

Correspondence
Jose Ivan Serrano-Contreras, Department of Metabolism, Digestion and Reproduction, Division of Digestive Diseases, Section of Nutrition, Faculty of Medicine, Imperial College London, Commonwealth Building, Hammersmith Campus, London W12 0NN, UK.
Email: j.serrano-contreras@imperial.ac.uk

Funding information
UK National Institute for Health Research; NIHR Imperial Biomedical Research Centre

Abstract

NMR spectroscopy is a mainstay of metabolic profiling approaches to investigation of physiological and pathological processes. The one-dimensional proton pulse sequences typically used in phenotyping large numbers of samples generate spectra that are rich in information but where metabolite identification is often compromised by peak overlap. Recently developed pure shift (PS) NMR spectroscopy, where all *J*-coupling multiplicities are removed from the spectra, has the potential to simplify the complex proton NMR spectra that arise from biosamples and hence to aid metabolite identification. Here we have evaluated two complementary approaches to spectral simplification: the HOBS (band-selective with real-time acquisition) and the PSYCHE (broadband with pseudo-2D interferogram acquisition) pulse sequences. We compare their relative sensitivities and robustness for deconvolving both urine and serum matrices. Both methods improve resolution of resonances ranging from doublets, triplets and quartets to more complex signals such as doublets of doublets and multiplets in highly overcrowded spectral regions. HOBS is the more sensitive method and takes less time to acquire in comparison with PSYCHE, but can introduce unavoidable artefacts from metabolites with strong couplings, whereas PSYCHE is more adaptable to these types of spin system, although at the expense of sensitivity. Both methods are robust and easy to implement. We also demonstrate that strong coupling artefacts contain latent connectivity information that can be used to enhance metabolite identification. Metabolite identification is a bottleneck in metabolic profiling studies. In the case of NMR, PS experiments can be included in metabolite identification workflows, providing additional capability for biomarker discovery.

KEYWORDS
band selective, broadband, metabolite identification, pure shift, strong coupling artefacts

Abbreviations: 1D, one dimensional; 2D, two dimensional; 4-CS, 4-cresyl sulfate; BB-PS, broadband pure shift; BS-PS, band-selective pure shift; HOBS, homodecoupled band-selective; *J*-Res, *J* resolved; NUS, non-uniform data sampling; PAG, phenylacetylglutamine; PS, pure shift; PSYCHE, pure shift yielded by chirp excitation; TMAO, trimethylamine *N*-oxide.

This is an open access article under the terms of the Creative Commons Attribution License, which permits use, distribution and reproduction in any medium, provided the original work is properly cited.
© 2023 The Authors. *NMR in Biomedicine* published by John Wiley & Sons Ltd.

1 | INTRODUCTION

Metabolic phenotyping aims to identify and quantify the metabolites present in biofluids such as urine or serum that are characteristic of different populations or patient groups. Phenotyping approaches are relevant to the investigation of case/control studies, identification of risk factors from epidemiological studies and exploration of the impact of nutritional differences on health outcomes.[1–4] The two main analytical approaches in metabolic phenotyping are NMR spectroscopy and mass spectrometry, the latter usually requiring a separation stage first, in either targeted or general profiling approaches. Whilst MS-based methods usually provide a wider coverage of the metabolic space and are more sensitive than NMR methods, NMR spectroscopy nevertheless remains a valuable tool because of its stability, the high degree of reproducibility and the large amount of molecular structural information within the spectrum. However, many metabolite NMR resonances are split into multiplets derived from coupled spins, which in turn causes substantial peak overlap. For instance, the spectral region between 3 and 4 ppm in urine and plasma contains multiple signals from carbohydrates, polyols and amino acids. Several approaches have been taken to reduce the spectral complexity, in particular *J*-resolved (*J*-Res) 2D spectroscopy, where the projection of the peaks on to the chemical shift axis yields singlet peaks for each multiplet (i.e., homodecoupling all of the spin coupled multiplets), thereby reducing the spectral region occupied by each metabolite.[5] In biofluid analysis, the *J*-Res experiment has typically been used to simplify urine and plasma spectra,[6] and has proved useful, for example, in the identification of inborn errors of metabolism[7,8] and in toxicology.[9,10] Whilst relatively rapid (requiring only 15 min to acquire both a standard one-dimensional (1D) spectrum and a *J*-Res spectrum[11]), the *J*-Res experiment is prone to generating spectral artefacts from strong coupling systems and lacks quantitation. Another approach to tackling the issue of overlapped signals is to acquire homo- or heteronuclear two-dimensional (2D) or even three-dimensional NMR experiments, but this requires extended experiment times and is therefore impractical to carry out for large cohorts of samples, even using non-uniform data sampling (NUS).[12]

Recently new NMR pulse sequences, using an approach termed pure shift (PS) NMR spectroscopy, have been developed to provide a single peak for each ^{1}H NMR spectral multiplet, which in turn has the potential to improve resolution in 1D spectra. Depending on the type of identification needed, using either the complete spectral window or a single region or signal, and the concentration of targeted metabolite (including known unknowns or unknown unknowns), broadband (BB-PS) or band-selective (BS-PS) experiments can be used. This is the case for the 1D pure shift yielded by chirp excitation (PSYCHE) experiment with pseudo-2D interferogram acquisition[13] and the 1D homodecoupled band-selective (HOBS) with real-time acquisition,[14] which are the most representative of the BB-PS and BS-PS methods, respectively. These methods are complementary due to the differences in their intrinsic properties. For instance, HOBS offers a reduction in experiment time compared with PSYCHE as the whole free induction decay is recorded at once instead of recording multiple data chunks in individual increments of a pseudo-2D spectrum,[15] but the former requires several experiments depending on the bandwidth used for homodecoupling whereas the latter covers the whole spectral window in one experiment. This is due to HOBS producing a spectrum for a signal or group of signals in a narrow band. Band-selective methods such as HOBS offer sensitivity higher than that of the BB-PS methods such as PSYCHE. However, PSYCHE is able to homodecouple strong coupling systems, but HOBS may show strong coupling artefacts. Despite their respective constraints, both methods produce ultrahigh-resolution spectra[14–18] that can be suitable to analyse complex mixtures. It is noteworthy that these two conventional PS methods only remove the effect of homonuclear HH couplings, and if other highly abundant active NMR nuclei are present in the molecular backbone such as ^{19}F or ^{31}P the effect of heteronuclear couplings is still present. A new PS method can remove all types of *J*-coupling.[19] However, heteronuclear *J*-couplings are rarely present in metabolic profiling studies using ^{1}H NMR spectroscopy, except in cases where fluorinated drugs and their metabolites are present, where phosphorylated compounds are detected or where isotopically labelled compounds have been used.

Here we evaluate the benefits and limitations of the two main published approaches based on the HOBS and PSYCHE pulse sequences by applying the methods to a variety of typical biofluid samples. We have also used a modification of the HOBS method called HOBS-PROJECT, where the CPMG-based PROJECT sequence is attached to the core HOBS pulse sequence to filter out the resonances from macromolecules such as proteins and lipoproteins,[20] which for samples such as serum/plasma can obscure the metabolite peaks. We illustrate the advantages of incorporating PS pulse sequences in a metabolite identification workflow using both urine and serum, which present different challenges in metabolic characterization.

1.1 | Experimental section

1.1.1 | Ethics and study design

We chose samples from a study that presented different analytical challenges that were relevant to the NMR experimental test parameters. Human samples were collected from healthy volunteers enrolled in a clinical trial for objective assessment of dietary patterns using metabolic phenotyping: a randomized, controlled, crossover trial. This study was approved by the London–Brent Research Ethics Committee and carried out in accordance with the Declaration of Helsinki (13/LO/0078). The study protocol has been published previously.[1] Samples collected included fasting serum samples, and urine samples.

10991492, 0, Downloaded from https://analyticalsciencejournals.onlinelibrary.wiley.com/doi/10.1002/nbm.5060 by National Health And Medical Research Council, Wiley Online Library on [08/11/2023]. See the Terms and Conditions (https://onlinelibrary.wiley.com/terms-and-conditions) on Wiley Online Library for rules of use; OA articles are governed by the applicable Creative Commons License

The analytical challenge of urine is that it is prone to change constantly as it is affected dynamically by hydration status, food intake and so on, and the number of metabolites found, including those of dietary and microbial origin, can amount to more than 3000.[21] Serum, with a smaller number of detectable metabolites and more physiologically stable than urine, has broad protein peaks that obscure the signals of small molecules. Moreover, both types of sample can generate spectra with overcrowded regions and dynamic range issues. Taking all of this into account, metabolite identification can be affected by these physicochemical properties, and thus new methodologies to tackle these issues could be beneficial to biomarker discovery.

1.1.2 | Sample preparation for NMR analysis

All samples were stored at −80 °C until analysis. Sample preparation is described in the Supporting Information. Briefly, urine and serum[11] samples were prepared for NMR-based metabolic profiling according to the literature.

1.1.3 | Conventional ^{1}H NMR spectroscopy

Urine-1, urine-4 and serum-1/2 samples were analysed on a Bruker 800 MHz Avance III HD spectrometer equipped with a 5 mm CPTCI *Z*-gradient cryoprobe and automated tuning and matching (Bruker BioSpin, Rheinstetten, Germany). Urine-2 and urine-3 samples were analysed on a Bruker 600 MHz Avance III HD spectrometer equipped with a 5 mm BBI *Z*-gradient probe and automated tuning and matching (Bruker BioSpin). The NMR spectra of urine samples were acquired at 300 K, and those for serum were acquired at 310 K. The samples were analysed with the pulse sequences and conditions normally used in high-throughput NMR-based metabolic profiling, with the only difference that extended versions of ^{1}H–^{1}H 2D *J*-Res experiment were used across the samples analysed.[11] From *J*-Res experiments the corresponding 1D projections (*pJ*-Res) were extracted using either the command 'proj' or 'f2projp' to calculate the positive partial projection. The parameter sets for acquisition and processing are described in the Supporting Information.

1.1.4 | BS-PS NMR spectroscopy

The 1D HOBS[14] and 1D HOBS-PROJECT[20] (serum-1 only) experiments with real-time acquisition and water pre-saturation during the relaxation delay were used as a BS-PS method. The parameter sets for acquisition and processing are described in the Supporting Information.

The 1D HOBS and the 1D HOBS-PROJECT pulse sequences are available on the Universitat Autònoma de Barcelona Servei de Ressonància Magnètica Nuclear Group website (SeRMN_UAB), (http://sermn.uab.cat/2015/05/lauracastanar-phdthesis/#more-3968).

1.1.5 | BB-PS NMR spectroscopy

The 1D PSYCHE (UoM_1d_if_psyche_ts4x)[13] experiment with pseudo-2D interferogram acquisition and water pre-saturation during relaxation delay was used as the BB-PS method. The parameter sets for acquisition and processing are described in the Supporting Information.

The 1D PSYCHE pulse sequence, the manual to explain the experiment and the automation processing programme are available on the Manchester NMR Methodology Group website (https://www.nmr.chemistry.manchester.ac.uk/?q=node/420).

For discussions regarding metabolite identification, HOBS and HOBS-PROJECT are referred to as BS-PS and PSYCHE as BB-PS experiments.

1.1.6 | Identification of metabolites

2D homonuclear and multiplicity-edited heteronuclear NMR experiments with water pre-saturation during the relaxation delay including gradient ^{1}H–^{1}H correlation spectroscopy 45° (cosygpprqf), ^{1}H–^{13}C heteronuclear single quantum coherence (hsqcedetgpsisp2.3) and ^{1}H–^{13}C heteronuclear multiple bond correlation (hmbcedetgpl3nd) were acquired for urine-1 and serum for identification purposes. The regular 1D selective TOCSY sequence (selmlgp) was also implemented for these samples. However, these data were not required to address the aim of this work, which is to assess the utility of the PS methods, and as such are not included.

Internal and external databases such as the Human Metabolome Data Base (HMDB; http://hmdb.ca/), the Biological Magnetic Resonance Data Bank (BMRB; http://www.bmrb.wisc.edu) or the Chenomx reference library (Chenomx NMR Suite 8.5, Edmonton, Alberta, Canada), and References 22–25, were used for confirmation of metabolite assignments.

10991492, 0, Downloaded from https://analyticalsciencejournals.onlinelibrary.wiley.com/doi/10.1002/nbm.5060 by National Health And Medical Research Council, Wiley Online Library on [08/11/2023]. See the Terms and Conditions (https://onlinelibrary.wiley.com/terms-and-conditions) on Wiley Online Library for rules of use; OA articles are governed by the applicable Creative Commons License

1.1.7 | Preparation of figures

The figures were made directly from TopSpin 3.6.1 without further manipulation of the spectra. GIMP 2.10.12 (http://www.gimp.org) was only used to increase the resolution of figures, and to label the signals from identified metabolites.

2 | RESULTS

2.1 | Performance of PS experiments

PS methods were compared with *pJ*-Res, where this approach proved to be more sensitive but have lower resolution than both PS approaches; within these, HOBS is more sensitive but with lower resolution than PSYCHE (Figures 1 and S2). On the other hand, the homodecoupling capacity was best performed by BB-PS: a number of artefacts from strong couplings appeared using BS-PS—for instance, from mutually coupled signals 4/4′, and 2/2′ of phenylacetylglutamine (PAG; see Figure 4 later).

PSYCHE performance was evaluated by changing the number of scans and data points. The best results were obtained using 112/128 scans and 64k data points per increment (Figure S1). The rationale for the implementation of 112 scans was to emulate the actual scenario where the need was to balance the parameters necessary to acquire homo- and heteronuclear 1D/2D NMR experiments for metabolite identification to save machine time and to collect good quality data. However, 2k data points per increment can be used as a starting point.

For HOBS experiments, where additional evaluation of different numbers of loops (L_0), acquisition times (AQ), bandwidths and offsets of the shaped pulse was conducted, best results were obtained using a pulse bandwidth of 0.5 ppm, acquiring around 32 different spectra in different chemical shift regions to cover the whole spectral window. Regarding the number of scans required, although a single scan could be sufficient to see homodecoupled signals (data not shown), 16 to 32 scans were used with a bandwidth of 0.5 ppm. More than 34 HOBS spectra may be needed to cover the whole spectral window instead of just the one spectrum needed for PSYCHE. It is worth noting that some signals including doublets and multiplets, mainly located in the aliphatic and carbohydrate region, started to be homodecoupled using 20 loops (L_0) and a bandwidth of 2 ppm, which were the same parameters as used to homodecouple resonances of cyclosporine.[14] In the case of HOBS-PROJECT, a bandwidth of 0.5 ppm also worked well with an acquisition time of 0.51 s, 32 loops, 16k data points and 16 scans. However, the best resolution was obtained with a bandwidth of 0.5 ppm, an acquisition time of 2.04 s, 70 loops, 64k data points and two scans (Figures 3 (later) and S15). In terms of data acquisition times, HOBS takes from 5 s to 1.5 min (one to 16 scans, respectively), whereas PSYCHE takes around 21 h.

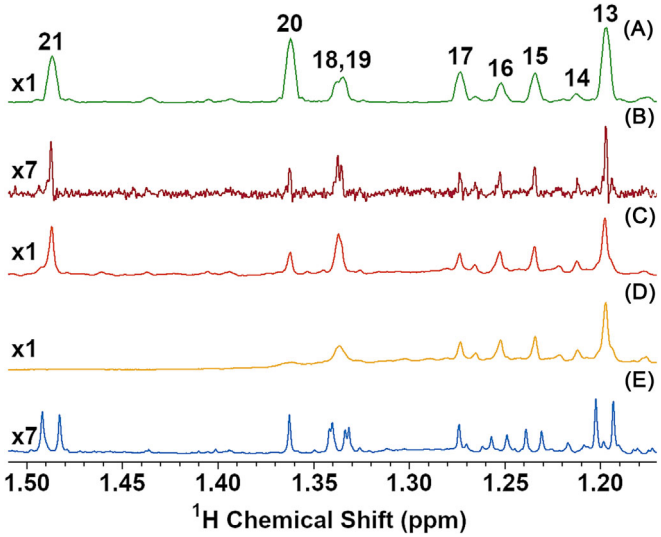


FIGURE 1 ^{1}H NMR spectra of urine-1 acquired at 800 MHz, comparing the sensitivity of the HOBS and PSYCHE pulse sequences with *pJ*-Res spectrum resulting from the corresponding 2D *J*-Res. A, *pJ*-Res; B, PSYCHE. C, D, HOBS using a 14.53 ms REBURP refocusing pulse to cover a bandwidth of 0.5 ppm (400 Hz), 32 scans and the offset set at 1.4 (C) or 1.15 (D) ppm. E, Regular 1D ^{1}H spectrum. SNR = 7085, 22, 516, 523 and 642 for A, B, C, D and E respectively using the resonance of 13 at 1.2 ppm as reference. Resolution (FWHM in Hz) using the same resonance: 4.1, 1.2, 2.8 and 2.7 for A, B, C and D, respectively. Key as indicated in Table 1. Vertical scales are indicated at the bottom left of the spectra.

10991492, 0, Downloaded from https://analyticalsciencejournals.onlinelibrary.wiley.com/doi/10.1002/nbm.5060 by National Health And Medical Research Council, Wiley Online Library on [08/11/2023]. See the Terms and Conditions (https://onlinelibrary.wiley.com/terms-and-conditions) on Wiley Online Library for rules of use; OA articles are governed by the applicable Creative Commons License

Regarding HOBS, two shapes of the selective pulse were tested using urine-2 only. Despite RSNOB being regarded as more selective than REBURP, the former gives results similar to those of REBURP with the parameters tested (Figures S2 and S3.1). Accordingly, we consistently adopted the pulse shape from the original paper of HOBS using REBURP[14] for analysis of the rest of the biosamples.

It was also observed that water suppression was an issue in regard to assigning signals close to the water resonance; this is more evident in BB-PS than in BS-PS (Figure S3). In the case of PSYCHE, regardless of the number of scans and data points collected, this issue is consistent in terms of amplitude and phase of the residual water (Figure S3.3).

2.2 | Strong coupling artefacts can aid metabolite identification

Regarding the strong coupling artefacts, even though the same sample was not acquired at both magnetic fields (i.e., 600 and 800 MHz), we can compare the behaviour of artefacts from some metabolites consistently present in urine under both magnetic fields. For instance, although urine-1 and urine-2 were not analysed with the same acquisition parameters, such as number of scans, both samples presented metabolites that showed the same artefacts in the *J*-Res spectra, attributed to metabolites such as 3-aminoisobutyrate, PAG, 4-cresyl sulfate (4-CS), citrate, serine and hippurate. The strong coupling artefact of citrate is the most evident at δ 2.62, where the signal is flanked symmetrically by its two corresponding doublets at δ 2.55 and δ 2.68. Another artefact flanked by two doublets (at δ 7.21 and δ 7.28) is from 4-CS at δ 7.24. The artefact of 3-aminoisobutyrate at δ 3.08 is flanked symmetrically by its two corresponding doublets of doublets at δ 3.04 and δ 3.11. Another artefact flanked by two doublets of doublets (at δ 3.96 and δ 4.00) is from serine at δ 3.98. Hippurate presents only one artefact at δ 7.60 flanked by two resonances at δ 7.56 and δ 7.64. In the case of PAG, it is possible to observe two overlapped artefacts at δ 7.40 (Figure 2).

Thus, the strong coupling artefacts in the *J*-Res/*pJ*-Res spectra are consistent regardless of the magnetic field strength used (Figure S4), indicating that the artefacts may be a reliable feature in terms of metabolite identification. In addition, conventional and NUS *J*-Res experiments were acquired for the same sample to confirm that NUS generates artefacts, and that artefacts from strong coupling effects are differentiated from those generated from NUS; this applies mostly to those metabolites at high concentration in either urine or serum (Figure S5).

There may be a dependence on the concentration of the metabolite or the nature of the nuclear system that causes artefacts to be observed or not in *J*-Res/*pJ*-Res spectra. Moreover, the strong coupling artefacts observed in *J*-Res/*pJ*-Res spectra match perfectly with those observed in PS spectra (Figures 2, 3, S4–S6, S8, S9, S11 and S14); all of them correspond to the same strong coupling artefacts.

These strong coupling artefacts can deliver connectivity information; for instance, phenylalanine in serum presents two artefacts corresponding to the aromatic moiety, where the one at δ 7.39 is more intense than that at δ 7.37 (Figure S6). The *ortho* coupling between Protons 1 and 2 produces an artefact with a bigger amplitude than that from the *ortho* coupling between Protons 1 and 3, possibly a consequence of the complex AA′BB′C spin system (Figure S6). These results open new leads for further research regarding spectral artefacts and connectivity information.

2.3 | Evaluation of the performance of PS NMR experiments for identifying specific metabolites in different biosamples

For discussions regarding metabolite identification, HOBS and HOBS-PROJECT are referred to as BS-PS and PSYCHE as BB-PS experiments. A wide range of metabolites was identified in each biofluid analysed. The representative signals from some of them were used to discuss our findings as most of them presented in good relative concentrations. In some of these cases, the output can be comparable between the two approaches used for homodecoupling regardless of the difference of sensitivity between BB-PS and BS-PS. However, for metabolites whose signals were close to the baseline, we will only discuss BS-PS as this approach is more sensitive than BB-PS.

For illustrative purposes, we have divided the spectrum into three main regions, named somewhat arbitrarily as aliphatic (from about 0.75 to 3.26 ppm), carbohydrate (from about 3.26 to 6 ppm) and aromatic (from about 6 to 10 ppm) regions. Regarding the carbohydrate region, we assigned signals as far as 6 ppm as some pentose sugars from nucleosides typically appear near there. However, within this region there exists a crowded zone with overlapping signals from about 3.26 to 4.30 ppm, where the 5-ribosyl moiety from pseudouridine normally appears, and the urea zone from about 5.65 to 5.90 ppm. Both zones are important to highlight the application of PS experiments on complex mixtures for metabolite identification as mentioned below. We describe our findings separately by biofluid.

2.3.1 | Urine

In urine-1, 71 metabolites were assigned Table 1). However, urine is highly variable in composition and thus the number of possible metabolites is far greater than that observed here. We only focus on metabolites that are illustrative from a PS point of view; most of these are related to dietary

10991492, 0, Downloaded from https://analyticalsciencejournals.onlinelibrary.wiley.com/doi/10.1002/nbm.5060 by National Health And Medical Research Council, Wiley Online Library on [08/11/2023]. See the Terms and Conditions (https://onlinelibrary.wiley.com/terms-and-conditions) on Wiley Online Library for rules of use; OA articles are governed by the applicable Creative Commons License

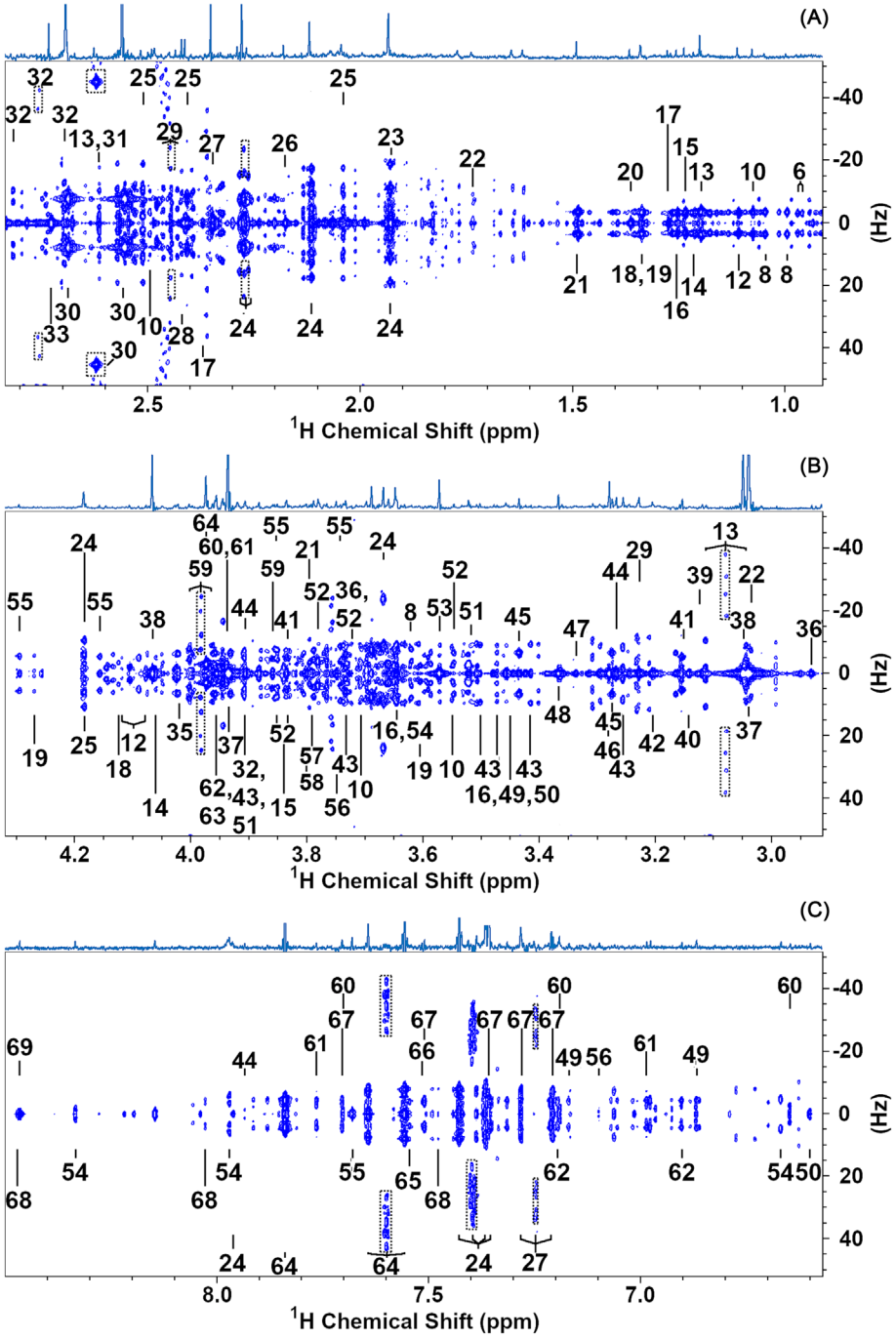


FIGURE 2 Conventional 2D *J*-Res spectrum of urine-1 acquired at 800 MHz with 1D PSYCHE spectrum plotted above showing the aliphatic (A), carbohydrate (B) and aromatic (C) regions. The dashed boxes indicate areas showing strong coupling artefacts. Key as indicated in Table 1.

intake and co-metabolism.[1] The aliphatic region from around 0.75 to 1.93 ppm is mainly comprised of resonances from metabolites that demonstrate singlets, doublets or triplets. Both BB-PS and BS-PS work to homodecouple the doublets and triplets in this zone (Figures 2A and S7). It was also noticed that resonances from lactate and threonine, which are typically overlapped in standard 1D spectra, can be properly resolved by PS approaches, in which BB-PS produces a more evident result in this regard (Figure S7.5–S7.6). The zone from around 1.93 to 3.26 ppm is comprised of more complex resonances, such that some of them produce strong coupling artefacts when trying to homodecouple them. For instance, PAG, carnitine, citrate, aspartate and 3-aminoisobutyrate have bands showing strong couplings in this zone, which BB-PS can deal with but BS-PS cannot (Figures 2A, B and S8.1). Despite the unavoidable presence of these strong coupling artefacts using BS-PS, it is possible to homodecouple them by moving the offset of the shaped pulse targeting the signal of interest as the case of citrate (Figure S8.2–8.3). However, citrate signals were homodecoupled by PSYCHE in one experiment (Figure 2A).

10991492, 0, Downloaded from https://analyticalsciencejournals.onlinelibrary.wiley.com/doi/10.1002/nbm.5060 by National Health And Medical Research Council, Wiley Online Library on [08/11/2023]. See the Terms and Conditions (https://onlinelibrary.wiley.com/terms-and-conditions) on Wiley Online Library for rules of use; OA articles are governed by the applicable Creative Commons License

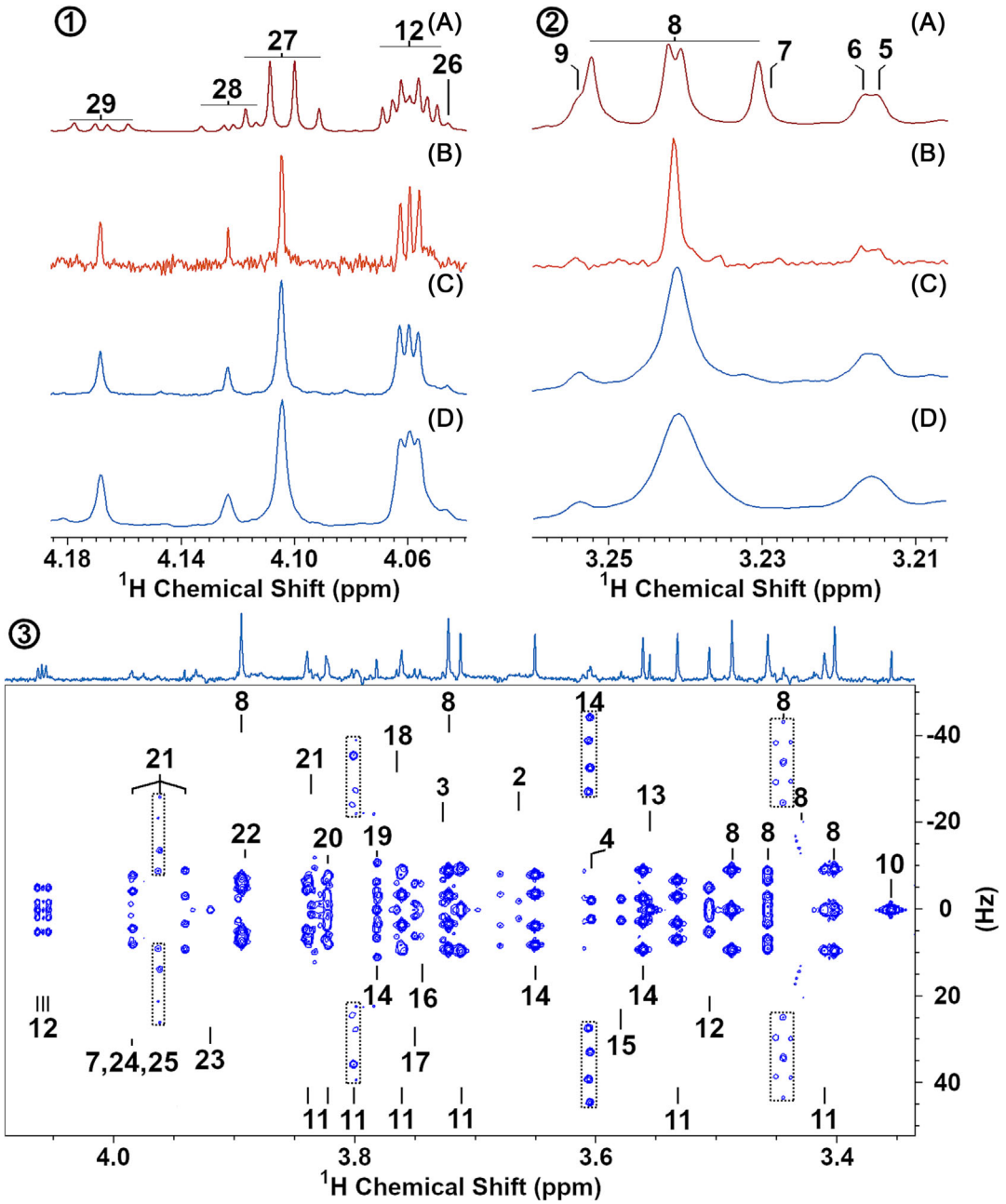


FIGURE 3 ^{1}H NMR spectra of a serum sample acquired at 800 MHz comparing the performance of the PSYCHE and the HOBS-PROJECT experiments. 1A, 1B, 2A, 2B, Standard ^{1}H CPMG spectrum (A) and PSYCHE (B) corresponding to the aliphatic (1) and carbohydrate (2) regions. 1C, 1D, 2C, 2D, HOBS-PROJECT using 14.53 ms REBURP refocusing pulse to cover a bandwidth of 0.5 ppm (400 Hz), an acquisition time (AQ) of 2.04 s (70 loops (L_0), 64k data points and 2 scans; C) or 0.51 s (L_0 of 32, 16k data points and 16 scans; D), a recycle delay (RD) of 4 s, the implementation of five loops for the T_2 filter (L_4), and the offset set at 4.25 (1) or 3.25 (2) ppm. Signal-to-noise ratio = 586, 17, 226 and 455 for 1A, 1B, 1C, and 1D, respectively using the resonance of 27 at 4.1 ppm as reference. Resolution (FWHM in Hz) using the same resonance: 1.1, 2 and 3.1 for 1B, 1C and 1D, respectively. SNR = 1171, 64, 408 and 896 for 2A, 2B, 2C and 2D, respectively using the resonance of 8 at 3.24 ppm as reference. Resolution (FWHM in Hz) using the same resonance: 1.3, 3.4 and 6 for 2B, 2C and 2D, respectively. 3, *J*-Res spectrum with 1D PSYCHE spectrum plotted above. The dashed boxes indicate areas showing strong coupling artefacts. Key as indicated in Table 2.

The carbohydrate region has signals that are both easy and difficult to homodecouple. Both BB-PS and BS-PS worked well; however, the former showed better results on homodecoupling strong couplings than the latter (Figures 2B and S9). BS-PS homodecoupled signals in this region, but the resultant singlets can be obscured by the artefacts of other signals with similar chemical shift but present in higher concentrations. In this context, it is difficult to distinguish between a real homodecoupled signal or an artefact. For instance, the two triplets at δ 4.16 and δ 4.29 of pseudouridine signals were homodecoupled by BB-PS (Figure 2B). This is less evident in BS-PS spectra, as these signals overlap with other

10991492, 0, Downloaded from https://analyticalsciencejournals.onlinelibrary.wiley.com/doi/10.1002/nbm.5060 by National Health And Medical Research Council, Wiley Online Library on [08/11/2023]. See the Terms and Conditions (https://onlinelibrary.wiley.com/terms-and-conditions) on Wiley Online Library for rules of use; OA articles are governed by the applicable Creative Commons License

TABLE 1 Peak assignments for identified metabolites in urine.

No.[a]	Urine no.	Metabolite	d[1]H [ppm]					
1	1	2-Methylbutyrate	0.86 (t)	1.06 (d)				
2	1	Fatty acids (C_n, n > 6)	0.88 (2 t)					
3	1	Valerate	0.89 (t)					
4	1	Isoleucine	0.94 (t)	1.01 (d)				
5	1	Ketoleucine	0.94 (d)					
6	1	Leucine	0.96 (d)	0.97 (d)				
7	1	2-Aminobutyrate	0.98 (t)	1.90 (m)				
8	1	Valine	0.99 (d)	1.04 (d)	3.62 (d)			
9	1	Propionate	1.06 (t)					
10	1	3-Hydroxyisobutyrate	1.08 (d)	2.5 (m)	3.55 (dd)	3.71 (dd)		
11	1	Isobutyrate	1.09 (d)					
12	1	4-Deoxyerythronate	1.11 (d)	4.07 (d)	4.12(m)			
13	1	3-Aminoisobutyrate	1.20 (d)	2.61 (m)	3.04 (dd)	3.08 (artefact)	3.11 (dd)	
14	1	a-Fucose	1.21 (d)					
15	1	4-Deoxythreonate	1.23 (d)	3.84 (d)	4.06 (m)			
16	1	b-Fucose	1.25 (d)	3.46 (m)	3.65 (dd)			
17	1	3-Hydroxyisovalerate	1.27 (s)	2.37 (s)				
18	1	Lactate	1.33 (d)	4.12 (q)				
19	1	Threonine	1.33 (d)	3.60 (d)	4.27 (m)			
20	1	2-Hydroxyisobutyrate	1.36 (s)					
21	1	Alanine	1.49 (d)	3.79 (q)				
22	1	Lysine	1.73 (m)	1.91 (m)	3.04 (t)			
23	1	Acetate	1.93 (s)					
24	1	PAG	1.93 (m, gem)	2.11 (m, gem)	2.26 (m, vic)	2.27 (artefact)	2.28 (m, vic)	3.65 (d)
			3.67 (q)	3.69 (d)	4.18 (m)	7.36 (m)	7.37 (m)	7.40 (artefact)
			7.43 (t)	7.97(m)				
25	1	Pyroglutamate (5-oxoproline)	2.03 (m)	2.41 (m)	2.51 (m)	4.18 (dd)		
26	1	*N*-Acetyl moiety	2.17 (s)					
27	1	4-CS	2.35 (s)	7.21 (d)	7.24 (artefact)	7.28 (d)		
28	1	Succinate	2.41 (s)					
29	1	Carnitine	2.43 (dd)	2.44 (artefact)	2.46 (dd)	3.23 (s)		
30	1	Citrate	2.55 (d)	2.62 (artefact)	2.69 (d)			
31	1	Methylamine	2.61 (s)					
32	1	Aspartate	2.69 (dd)	2.75 (artefact)	2.81 (dd)	3.91 (dd)		
33	1	Dimethylamine	2.73 (s)					
34	1	1-Methylguanidine	2.83 (s)					
35	1	Asparagine	2.88 (dd)	2.96 (dd)	4.01 (dd)			
36	1	Dimethylglycine (DMG)	2.93 (s)	3.73 (s)				
37	1	Creatine	3.04 (s)	3.93 (s)				
38	1	Creatinine	3.05 (s)	4.06 (s)				
39	1	*Nε*,*Nε*,*Nε*-Trimethyllysine	3.12 (s)					
40	1&2	*cis*-Aconitate	3.14 (d)	5.79 (m)				
41	1	Ethanolamine	3.15 (t)	3.83 (t)				
42	1	Choline	3.20 (s)					
43	1	β-Glucose	3.26 (dd)	3.41 (m)	3.47 (m)	3.50 (t)	3.73 (dd)	3.91 (dd)
44	1	Betaine	3.27 (s)	3.90 (s)				
45	1	Taurine	3.28 (t)	3.43 (t)				
46	1	TMAO	3.28 (s)					
47	1	*scyllo*-Inositol	3.35 (s)					
48	1	Methanol	3.37 (s)					

10991492, 0, Downloaded from https://analyticalsciencejournals.onlinelibrary.wiley.com/doi/10.1002/nbm.5060 by National Health And Medical Research Council, Wiley Online Library on [08/11/2023]. See the Terms and Conditions (https://onlinelibrary.wiley.com/terms-and-conditions) on Wiley Online Library for rules of use; OA articles are governed by the applicable Creative Commons License

TABLE 1 (Continued)

No.[a]	Urine no.	Metabolite	d[1]H [ppm]					
49	1	2-(4-Hydroxyphenyl)acetate (4-Hydroxyphenylacetate)	3.45 (s)	6.87 (d, AA′BB′)	7.17 (d, AA′BB′)			
50	1	*trans*-Aconitate	3.46 (d)	6.60 (m)				
51	1	Arabinose	3.51 (dd)	3.91 (dd)				
52	1&3	α-Glucose	3.55 (dd)	3.72 (dd)	3.78 (m)	3.83 (m)	3.85 (m)	
53	1	Glycine	3.57 (s)					
54	1	*N* [1]-Methyl-2-pyridone-5-carboxamide	3.65 (s)	6.67 (dd)	7.97 (dd)	8.33 (d)		
55	1	Pseudouridine	3.74 (m)	3.85 (m)	4.02 (m)	4.16 (t)	4.29 (t)	7.68 (d)
56	1	1-Methyl-histidine	3.75 (s)	7.10 (d)	7.93 (d)			
57	1	3-Methyl-histidine	3.79 (s)					
58	1	Guanidoacetate	3.80 (s)					
59	1	Serine	3.86 (dd)	3.96 (dd)	3.98 (artefact)	4.00 (dd)		
60	1	2-Furoylglycine	3.94 (d)	6.65, (dd)	7.19 (dd)	7.70 (dd)		
61	1	4-Hydroxy-hippurate	3.94 (m)	6.99 (d, AA′BB′)	7.76 (d, AA′BB′)			
62	1	Tyrosine	3.95 (dd)	6.90 (d, AA′BB′)	7.19 (d, AA′BB′)			
63	1	Glycolate	3.95 (s)					
64	1	Hippurate	3.97 (d)	7.56 (t)	7.6 (artefact)	7.64 (t)	7.84 (m)	8.52 (br)
65	1&2	Uracil	5.81 (d)	7.55 (d)				
66	1	Cytosine	5.98 (d)	7.52 (d)				
67	1	3-Indoxylsulfate	7.21 (ddd)	7.28 (ddd)	7.36 (s)	7.51 (d)	7.70 (d)	
68	1	Quinolinate	7.47 (dd)	8.03 (dd)	8.47 (dd)			
69	1	Formate	8.46 (s)					
70	1	*N*-Methylnicotinate (trigonelline)	8.84 (m)	8.85 (m)	9.12 (s)			
71	1	1-Methylnicotinamide	8.90 (d)	8.97 (d)	9.28 (s)			
72	2	Acesulfame	2.128 (d)	5.68 (m)				
73	3	Acetaminophen glucuronide	5.11 (d)	7.15 (d, AA′BB′)	7.37 (d, AA′BB′)			
74	3	Acetaminophen sulfate	7.32 (d, AA′BB′)	7.39 (artefact)	7.46 (d, AA′BB′)			

[a]Number is related to the labels in the figures corresponding to urine samples. Metabolites are ordered based on chemical shifts observed in urine-1. Multiplicity key: s = singlet, d = doublet, t = triplet, q = quartet, m = (other) multiplet, dd = doublet of doublets, ddd = doublet of doublet of doublets, br = broad signal; gem = geminal and vic = vicinal protons observed via gCOSY45. AA′BB′ spin system. Peaks resolved by **BS-PS (blue)**, **BB-PS (green)** or **both (purple)**. *J*-Res confirmed the strong coupling artefacts for all metabolites that presented them. Acesulfame, acetaminophen glucuronide and acetaminophen sulfate are xenometabolites: their presence in urine, and detection by NMR spectroscopy, depends on the participant exposure.

resonances (Figure S9.3–S9.6). The artefacts observed in the carbohydrate region derived mainly from diastereotopic protons of metabolites such as amino acids, carbohydrates and those that have an amino acid or carbohydrate or any substituent that provides a chiral moiety in their chemical backbone. For instance, although the PAG signal at δ 3.67 produced an unavoidable artefact whilst using BS-PS (Figure S9), it was fully homodecoupled by BB-PS (Figure 2B). In contrast, the resonance of PAG at δ 4.18 was homodecoupled by both approaches. However, neither approach could differentiate the isochronic signals from PAG and pyroglutamate at this chemical shift (Figures 2B and S9.5–9.6).

The confirmation of the presence of singlets in this crowded region was also possible using PS approaches. This was also assessed using a *J*-Res spectrum along with PS. For instance, the presence of the singlet of carnitine that overlaps with the doublet of doublets of 1-methyl-histidine at δ 3.23 was confirmed using HOBS (Figure S9.1–S9.2). In this context, with the offset of the shaped pulse at an appropriate position to homodecouple the signal of β-glucose at δ 3.26, it was possible to resolve the singlet from the homodecoupling of the signal of taurine, and the two singlets from betaine and trimethylamine *N*-oxide (TMAO) (Figure S9.1–9.2). Other singlets that were appropriately resolved in the carbohydrate region were those corresponding to 1-methyl-histidine, guanidinoacetate and glycolate (Figure S9.3–9.6). Singlets were also resolved by PSYCHE; however, their corresponding metabolites should be at high concentration (Figure 2B). Within the carbohydrate region and close to the aromatic region exists the urea zone in which the signal of urea obscures resonances of other metabolites such as *cis*-aconitate, uracil and cytosine. However, the homodecoupling of their corresponding resonances were properly observed using BS-PS (Figure S10.1–10.2).

The aromatic region also contains a mixture of signals, some of which are easy, and some of which are difficult to homodecouple. For instance, the signals of *trans*-aconitate, 2-furoylglycine, *N* [1]-methyl-2-pyridone-5-carboxamide, 2-(4-hydroxyphenyl)acetate

10991492, 0, Downloaded from https://analyticalsciencejournals.onlinelibrary.wiley.com/doi/10.1002/nbm.5060 by National Health And Medical Research Council, Wiley Online Library on [08/11/2023]. See the Terms and Conditions (https://onlinelibrary.wiley.com/terms-and-conditions) on Wiley Online Library for rules of use; OA articles are governed by the applicable Creative Commons License

(4-hydroxyphenylacetate), tyrosine, 4-hydroxy-hippurate and 1-methyl-histidine, which appear in the region that ranges from about 6.60 to 7.10 ppm, were homodecoupled by both PS approaches (Figures 2C and S10.3–10.6). A more complex zone from the aromatic region could be found from about 7.19 to 7.85 ppm, where the predominant resonances correspond to 4-CS, PAG and hippurate. These signals originate from strong couplings from symmetrical spin systems, being more evident in the corresponding *J*-Res spectrum, which resulted in being homodecoupled by BB-PS, but with artefacts using BS-PS (Figure 2C and Figure S11). The signals of hippurate at δ 7.56 and δ 7.84 were the only ones that were homodecoupled by BS-PS (Figure S11.1).

4-CS and PAG artefacts obscure the resonances of 3-indoxyl sulfate at δ 7.21, δ 7.28 and δ 7.36, and it is not possible to say accurately whether homodecoupling took place for these signals or not, particularly for BS-PS. However, the other two resonances of 3-indoxyl sulfate at δ 7.51 and δ 7.70 were homodecoupled and resolved by this PS method (Figure S11.1). The implementation of BS-PS made it possible to observe some signals with low intensity and their behaviour under this approach, which was not possible with BB-PS. For instance, the doublet of 1-methyl-histidine at δ 7.93 was homodecoupled. In the case of N^1-methyl-2-pyridone-5-carboxamide, there was clear evidence of homodecoupling of the signal at δ 8.33 (Figure S12.1–12.2), but whether homodecoupling for the resonance at δ 7.97, which overlaps with a singlet and the signal from the –NH proton of PAG, occurred or not was not apparent. We identified the signals from *N*-methylnicotinate (trigonelline) and 1-methylnicotinamide: these metabolites are normally at low concentration in urine samples. Nevertheless, with BS-PS was possible to observe and homodecouple their signals, and to resolve the two overlapped resonances of trigonelline at δ 8.84 and δ 8.85. It is of note that these signals were not properly observed by *J*-Res (Figure S12.3–12.4).

In addition to the urine sample analysed at 800 MHz, we also measured two urine samples (2 and 3) that were known to contain metabolites of certain xenobiotics. These were measured at 600 MHz to evaluate the performance of BS-PS on targeted resonances corresponding to the metabolites of acesulfame-K and acetaminophen. Acesulfame-K has two signals, one in the urea zone, and one in the aliphatic region, both of which were homodecoupled and resolved by BS-PS (Figure S13). Regarding acetaminophen, it was possible to homodecouple the AA′BB′ spin systems derived from the *p*-disubstituted benzene ring moieties that belong to acetaminophen glucuronide and sulfate (Figure S14.1). Despite the higher relative concentration of the acetaminophen glucuronide over the sulfate, the artefact from the former at δ 7.26 in the *J*-Res spectrum is less intense than that from the latter at δ 7.39 (Figure S14.3). Moreover, the doublet at δ 5.11 of the glucuronic acid moiety was also homodecoupled (Figure S14.2 and S14.4), and possible to observe despite the issue of water saturation (Figure S3.2).

2.3.2 | Serum

In serum, a total of 29 metabolites were assigned in serum-1 (Table 2). Serum is a biomatrix with a high concentration of proteins, whose broad peaks obscure those from metabolites. The PROJECT approach, similar to the CPMG experiment, suppresses the signals of proteins, and when it is conjugated to BS-PS it is possible to obtain clearer homodecoupled spectra without the broad signals from proteins. Although BS-PS without PROJECT was also able to produce homodecoupled spectra, suppression of the protein signals allows for easier assignment of metabolites. This is exemplified when comparing representative zones of the aliphatic and aromatic regions, in which we used different numbers of loops and scans for homodecoupling: BS-PS was able to homodecouple and resolve the signals, however, against the background of protein resonances. Moreover, when PROJECT is coupled to BS-PS, there must be a trade-off between sensitivity and resolution in order to choose appropriate parameter sets to deliver the desired results (Figure S15). For the present study, we did not try to compare the two T_2 filters to supress protein signals. CPMG is normally acquired for blood samples in metabolic profiling for this purpose. PROJECT is a pulse sequence based on CPMG and has been attached to the HOBS sequence to measure T_1 and T_2 relaxation times from overlapped resonances.[20] Taking advantage of this, we used BS-PS (HOBS-PROJECT) to analyse serum to homodecouple signals from small molecules, and to suppress protein signals at the same time. This capability gives this BS-PS approach the potential to identify metabolites in both serum and plasma. In this context, and as described for previous samples, the carbohydrate region is compromised by crowding with overlapping signals from multiple metabolites, and serum is not an exception. However, serum is one of the most homogenous types of biofluid sample, in concentration terms, in which the resonances from α-glucose and β-glucose predominate in the carbohydrate region, making it difficult to assign other metabolites whose resonances appear in this region. The best performance in simplifying this region was achieved by BB-PS, which was able to homodecouple and resolve the signals of α-glucose, β-glucose, isoleucine, leucine, valine, glycerol, threonine, lysine, glutamate, alanine and serine in one experiment. Nonetheless, BS-PS was also useful for homodecoupling signals and resolved some multiplets in this region such as the signals of choline, proline and pyroglutamate. Despite NMR spectral singlets from metabolites or moieties with uncoupled spins being unaffected by PS, their differentiation from other singlets derived from homodecoupling of coupled spin systems by PS is essential, as metabolites with actual singlets are problematic to annotate. In this context, both PS methods were able to differentiate singlets in the carbohydrate region. This is the case for carnitine, phosphorylcholine, betaine, methanol, choline, glycine and creatine. Choline was a particular case that produced a pseudotriplet (i.e., three singlets) using both PS approaches; this could be derived from the three methyl groups attached to the quaternary nitrogen (Figure 3).

10991492, 0, Downloaded from https://analyticalsciencejournals.onlinelibrary.wiley.com/doi/10.1002/nbm.5060 by National Health And Medical Research Council, Wiley Online Library on [08/11/2023]. See the Terms and Conditions (https://onlinelibrary.wiley.com/terms-and-conditions) on Wiley Online Library for rules of use; OA articles are governed by the applicable Creative Commons License

TABLE 2 Peak assignments for identified metabolites in serum.

No.[a]	Metabolite	d^{1}H [ppm]							
1	Lipoproteins[b]	0.83–0.89 (br)							
2	Isoleucine	0.93 (t)	1.00 (d)	3.66 (d)					
3	Leucine	0.95 (d)	0.96 (d)	3.73 (m)					
4	Valine	0.98 (d)	1.03 (d)	3.60 (d)					
5	Carnitine	3.21 (s)							
6	Phosphorylcholine	3.22 (s)							
7	Histidine	3.23 (dd)	3.98 (dd)	7.06 (s)	7.80 (s)				
8	β-Glucose	3.24 (dd)	3.40 (m)	3.42 (artefact)	3.44 (artefact)	3.45 (m)	3.48 (t)	3.72 (dd)	3.90 (dd)
9	Betaine	3.25 (s)							
10	Methanol	3.36 (s)							
11	α-Glucose	3.41 (m)	3.53 (dd)	3.71 (dd)	3.76 (m)	3.80 (artefact)	3.82 (m)	3.84 (m)	
12	Choline	3.50 (m)	4.06 (3 m)						
13	Glycine	3.55 (s)							
14	Glycerol	3.56 (dd)	3.60 (artefact)	3.65 (dd)	3.78 (m)				
15	Threonine	3.58 (d)							
16	Albumin lysyl	3.74 (t)							
17	Glutamate	3.75 (dd)							
18	Lysine	3.76 (t)							
19	Alanine	3.78 (q)							
20	Ethanolamine	3.82 (m)							
21	Serine	3.84 (m)	3.94 (dd)	3.96 (artefact)	3.98 (dd)				
22	Methionine	3.88 (dd)							
23	Creatine	3.92 (s)							
24	1,5-Anhydro-D-glucitol	3.97 (dd)							
25	Phenylalanine	3.28 (dd)	3.98 (dd)	7.32 (m)					
26	Creatinine	4.04 (s)							
27	Lactate	4.10 (q)							
28	Proline	4.12 (m)							
29	Pyroglutamate (5-oxoproline)	4.17 (m)							
30	Tyrosine	7.19 (d), AA′BB′							
31	Unknown	7.32 (s)							

Note: Multiplicity key is as follows: s = singlet, d = doublet, t = triplet, q = quartet, m = (other) multiplet, dd = doublet of doublets. AA′BB′ spin system. Peaks resolved by **BS-PS (blue)**, **BB-PS (green)** or **both (purple)**. *J*-Res confirmed the strong coupling artefacts for all metabolites that presented them.

[a]Number is related to the labels in the figures corresponding to serum.

[b]Signals from terminal methyl-group protons.

3 | DISCUSSION

The homodecoupling power and the sensitivity achieved using BB-PS and BS-PS pulse sequences were consistent with previous work reported in the literature. For instance, BB-PS was shown to be more tolerant to strong couplings but with the cost of lower sensitivity. In contrast, BS-PS has better sensitivity but was associated with the appearance of strong coupling artefacts, other artefacts or signals that have not been homodecoupled.[14–18]

It is evident that for strong couplings BB-PS works better than BS-PS as observed for the complex multiplets arising from carbohydrates and aromatic moieties, which in turn made it possible to tackle the issue of overlapped signals in these regions (Figures 2–4 and S9–S11). On the other hand, BS-PS is more sensitive than BB-PS, which makes it a potential tool to analyse and identify metabolites at low concentration in a given sample (Figures S12 and S13). Thus, running only BS-PS might be sufficient to save time, producing useful data for metabolite identification. This is in order to know how many signals are going to be selected for identification purposes, as it could be the case that it might be possible not to cover the complete spectral window but only to focus on certain target signals.

In addition, the inherent low sensitivity of BB-PS and the issue due to the residual water signal from water suppression during the relaxation delay means that it is not possible to observe resonances close to the water peak. However, using BS-PS, it was possible to observe

10991492, 0, Downloaded from https://analyticalsciencejournals.onlinelibrary.wiley.com/doi/10.1002/nbm.5060 by National Health And Medical Research Council, Wiley Online Library on [08/11/2023]. See the Terms and Conditions (https://onlinelibrary.wiley.com/terms-and-conditions) on Wiley Online Library for rules of use; OA articles are governed by the applicable Creative Commons License

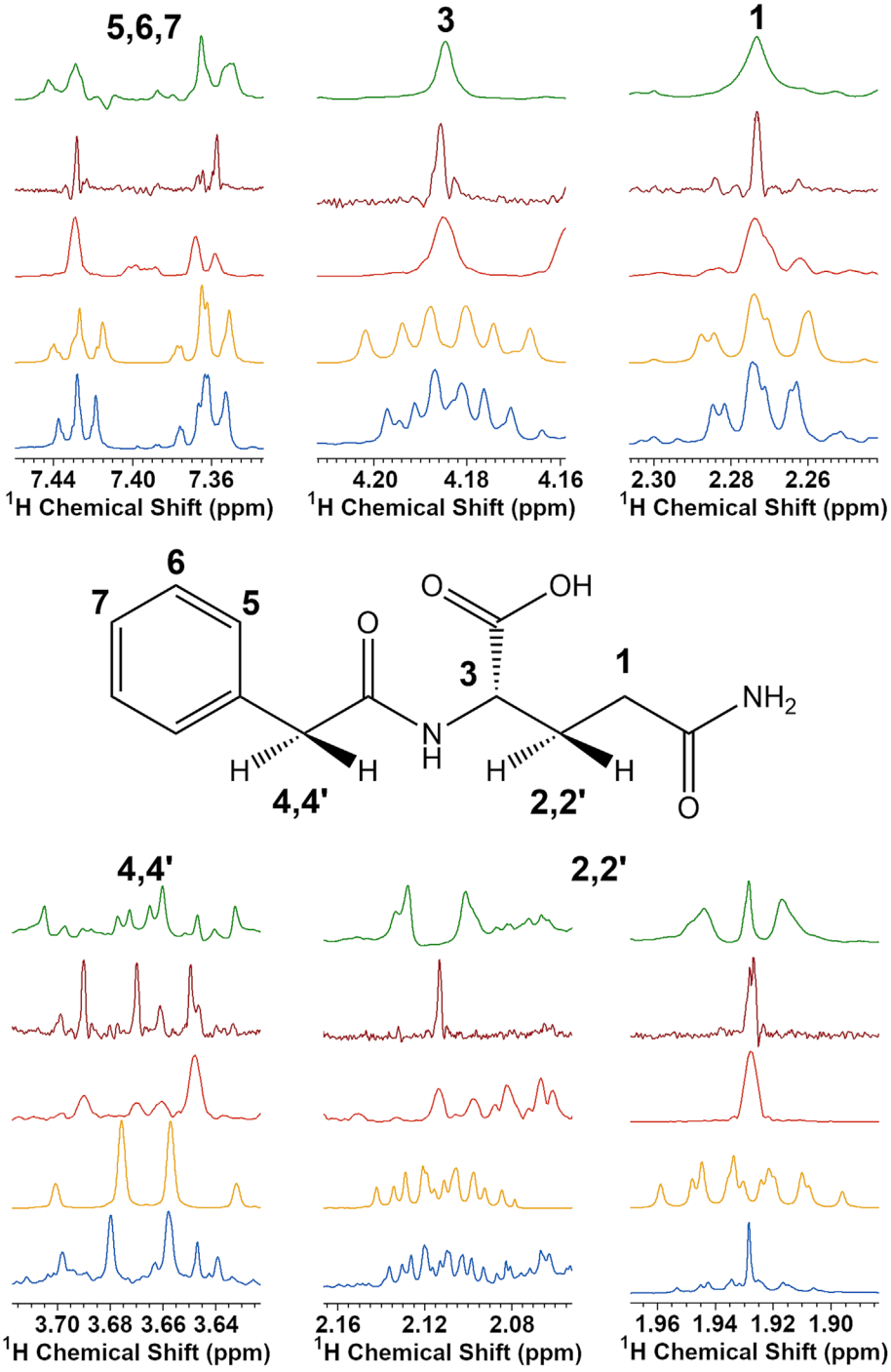


FIGURE 4 Blue, orange, red and green, peak assignments of PAG using PS experiments from untargeted analysis of urine-1 at 800 MHz: 1D ^{1}H NMR, *pJ*-Res, PSYCHE and HOBS spectra respectively. Yellow, 1D ^{1}H NMR spectrum of an aqueous solution with the authentic standard of PAG (4.7 mM) acquired at 600 MHz. HOBS spectra shown here were acquired using a 14.53 ms REBURP refocusing pulse to cover a bandwidth of 0.5 ppm (400 Hz), 16 scans, with the offset set at 2, 2.4, 3.65, 4.4 and 7.4 (for protons 2 and 2′, 1, 4 and 4′, 3, and 5, 6 and 7, respectively).

homodecoupling of targeted signals close to the water residual resonance, including for instance, the anomeric protons of α/β-anomers of carbohydrates and the resonance of acetaminophen glucuronide at δ 5.11. Moreover, the zone from 3.26 to 4.3 ppm is the most compromised, as it is comprised of overlapped signals with large concentration range differences among the metabolites whose resonances appear in this zone. Accordingly, PS approaches can aid the resolution of the signals in this zone to facilitate metabolite identification. In terms of numbers, those signals that appear in the conventional 1D ^{1}H spectrum close to the residual water peak within the range between 4.6 and 5 or 4.4 and 5.2 ppm can be lost due to the water issue observed in BS-PS and BB-PS respectively.

10991492, 0, Downloaded from https://analyticalsciencejournals.onlinelibrary.wiley.com/doi/10.1002/nbm.5060 by National Health And Medical Research Council, Wiley Online Library on [08/11/2023]. See the Terms and Conditions (https://onlinelibrary.wiley.com/terms-and-conditions) on Wiley Online Library for rules of use; OA articles are governed by the applicable Creative Commons License

The capacity of HOBS to homodecouple targeted resonances of metabolites in biofluids is made possible by changing the bandwidth of the refocusing pulse and/or changing the offset to ensure that non-mutually coupled signals are excited within the same bandwidth. In the first case, reducing the bandwidth to 0.5 ppm gave the best results. However, BS-PS was also able to homodecouple some signals by using a bandwidth of 1 and even 2 ppm if no mutually coupled signal were in the selected area. In the second case, BS-PS should be acquired with the selective pulse applied in the middle of the targeted region or signal to be decoupled. For this purpose, *J*-Res can be used as guidance to centre the shaped pulse on the targeted region/signal of the metabolite to identify.

BB-PS can work better for strong couplings than BS-PS, although the metabolite in question needs to be at a high concentration to provide a detectable signal by this approach. It is possible to tackle the issue of concentration, to some extent, by choosing the sample with the highest relative concentration of the targeted metabolite(s) from the batch of samples analysed for a given project. Another alternative is to concentrate the sample in question to be able to use BB-PS with a more practical experiment time.

The implementation of the PROJECT element attached to the HOBS pulse sequence enables the suppression of signals from proteins and in turn makes it possible to implement this homodecoupling approach for metabolite identification for analysis of serum/plasma or samples with a high level of protein or other macromolecules. On the other hand, PSYCHE did not require a mechanism for suppressing the signals from proteins as it could produce a metabolite spectrum clear of protein signals. This is because the PSYCHE pulse sequence element acts as a T_2 filter on its own due to its long duration (i.e., tens of milliseconds).[26]

In general, the aspects to be considered before running PS experiments for metabolite identification purposes are the following.

1. Type of biofluid to be analysed. Some biofluids are naturally more concentrated than others. For instance, urine samples from well hydrated subjects can be quite dilute.
2. Concentration of the analyte in the sample. Normally a sample with the highest concentration of the metabolite from the cohort under study is used. If it is possible to collect a large sample volume, it is advisable to concentrate the sample prior to conducting NMR analysis for identification purposes.
3. Experiment time. BB-PS takes longer than BS-PS. For the latter, around 34 spectra (sample dependent) are needed to cover the complete spectral width normally used in metabolic profiling (e.g., about 9–10 ppm), which would take around 54 min if 16 scans per region were used. In the case where only a specific area, zone or resonance is required to be analysed, in a targeted or semi-targeted approach as for spiking assays, the experiment time can be reduced to a few minutes. This might be helpful if the analysis is set to automation mode. Accordingly, one scan may be sufficient to check the performance of BS-PS on targeted signal(s) before running the actual analysis.
4. Targeted signals may be known a priori during the high-throughput analysis of a given sample cohort (i.e., signals observed in previous analyses from similar projects) or a posteori with statistical approaches such as STOCSY or STORM.[27,28] This will depend on the experience of the analyst.

It was evident that there were many unassigned metabolites present in all matrices analysed in the present study. Thus, for illustrative purposes only metabolites with confirmed assignments were depicted in the figures to highlight which metabolites presented homodecoupled signals and which ones showed strong coupling artefacts in PS spectra. The strong coupling artefacts observed in these spectra were foreseeable from *J*-Res spectra. This means that *J*-Res can produce a priori information about which signals tend to produce strong coupling artefacts in PS spectra. In general, since the presence of strong coupling artefacts is unavoidable, their presence in a *J*-Res spectrum can be used as an extra tool for metabolite identification by using the shape of the signals, their chemical shifts and the symmetry/pattern of the resulting artefact. However, using strong coupling artefacts observed in the *J*-Res spectrum for metabolite identification should be done with caution to avoid confusion over whether the signal in the middle is an actual artefact of its corresponding metabolite or a real signal from another metabolite, or if the artefact overlaps with another resonance. It is possible to see if a signal will result in an artefact in PS experiments by looking at the corresponding resonances in the *J*-Res spectrum, in which it is possible to observe the artefact in the middle of the resonances from which it derives (which may be referred as the two parent resonances).

In this context, we found that strong coupling artefacts observed in *J*-Res spectra that could produce strong coupling artefacts in PS spectra were, in general, from resonances related to geminal protons, *p*-disubstituted phenyl moieties and monosubstituted phenyl moieties, plus in addition, specifically, strong coupling artefacts derived from vicinal protons observed for β-glucose. Thus, the analysis of these artefacts can be used as connectivity information, which makes it a potential tool for metabolite identification. This could also be very useful in overcrowded zones, as these artefacts in *J*-Res spectra are observed as 'signals' with splittings more than 40 Hz apart (i.e., 20 Hz on each side of the second dimension in a *J*-Res spectrum). If possible, the *J*-Res from the actual standard could be used as template to trace and confirm the presence of the strong coupling artefact in question. In this context, only the most intense artefacts observed in *J*-Res spectra are illustrated in the corresponding figures. However, we found that more artefacts from metabolites at low concentration start to appear when scaling up the intensity of the *J*-Res spectra.

Another illustrative instance of using strong coupling artefacts in *J*-Res spectra is the identification of serine, which was found in both urine and serum. In this context, due to its resonances being hidden in a highly crowded spectral region, specifically the carbohydrate region, it is possible that many studies to date have not identified this metabolite as significant, as statistical analyses are normally performed on 1D ^{1}H NMR spectra. This may have an impact on the biological interpretation, as serine has been related to cancer, brain and central nervous system development

10991492, 0, Downloaded from https://analyticalsciencejournals.onlinelibrary.wiley.com/doi/10.1002/nbm.5060 by National Health And Medical Research Council, Wiley Online Library on [08/11/2023]. See the Terms and Conditions (https://onlinelibrary.wiley.com/terms-and-conditions) on Wiley Online Library for rules of use; OA articles are governed by the applicable Creative Commons License

and disorders.[29–32] This makes it attractive to be more cautious in analysing this metabolite in epidemiological studies. One approach to circumventing this issue could be extracting serine resonances from the *J*-Res spectra and analysing them separately as a targeted approach.

In addition to endogenous metabolites, it is possible to observe widely used xenobiotics and their xenometabolites, but although common they should not be expected in every sample.[22] Hence the importance of their identification, where artefacts observed in *J*-Res spectra can provide structural information to identify them in biofluids: for instance, in the comparison between acetaminophen glucuronide (g-APAP) and acetaminophen sulfate (s-APAP), in which, despite the higher relative concentration of g-APAP in comparison to s-APAP, the latter exhibits more intense strong coupling artefacts than those of g-APAP. This is also evident in p-CS, which also has an AA′BB′ spin system. Thus, by looking for the presence of AA′BB′ spin systems from *p*-disubstituted aromatic rings in the *J*-Res spectra, it may be possible to infer whether an *O*-glucuronide or *O*-sulfate moiety is attached to the aromatic ring.

Acesulfame is another xenometabolite that is unmetabolized prior to its rapid excretion in urine and has been regarded as a biomarker of medications, dental preparations and dietary intake of products that contained it such as carbonated beverages and processed foods.[33–35] This artificial sweetener has been detected by 1D ^{1}H NMR spectroscopy in urine from healthy participants.[36]

A summary of the metabolites with their corresponding moieties that produce strong coupling artefacts observed in *J*-Res spectra are reported in Table S1.

The implementation of PS experiments in assigning metabolite peaks in the present study was also assisted by *J*-Res and conventional 1D-selective TOCSY spectra. These experiments provide additional information with short data acquisition times. Thus, these experiments can be regarded as complementary for metabolite identification in complex mixtures, making it possible to target only the signal(s) of unknown metabolite(s) at lower concentrations for assignment. However, homonuclear and heteronuclear 2D NMR experiments are also important for confirmation of the assignments. In this context, the worst case scenario for PS experiments in terms of identification purposes is where the target metabolite is at a lower concentration than other metabolites that have similar chemical shifts. The situation worsens when the overlapped metabolites at higher concentrations produce strong coupling artefacts and/or the metabolite to be identified produces them. This applies to *p*-CS, whose signals are more intense than 3-indoxyl sulfate signals, which produce strong coupling artefacts using BS-PS. Conversely, BB-PS was able to homodecouple and resolve the signals from both metabolites (Figure 2C).

Another clue to assign signals that are overlapped and that are difficult to assign even in PS spectra is the possibility to use *J*-Res spectra by looking at the intensity that should correspond to the one in the PS spectra, and also the shape and symmetry of the resonance in question. This is the case for 4-hydroxyphenylacetate, whose resonance at δ 6.87 ppm corresponds to a doublet from an AA′BB′ spin system, which has the characteristic shape of this type of spin system in the *J*-Res spectrum and it is also more intense than the closest signal at highest field (Figure S10.6).

One of the virtues of NMR spectroscopy is that some metabolites have resonances at different chemical shifts that may appear in different regions. Thus, it is possible to target a representative signal that perfectly homodecouples and whose chemical shift appears in a non-crowded zone. PAG is the best instance of this, as it has signals in the three regions mentioned earlier, but only one signal can be regarded as a representative signal for this metabolite. This is the multiplet at δ 4.18, which is homodecoupled by both approaches, BB-PS and BS-PS, and located in a non-overcrowded zone. The other PAG resonances show strong couplings, where BB-PS can work (Figure 4). Other instances are the multiplets of proline (in serum) and pyroglutamate (in urine and serum), whose resonances in the aliphatic region produce strong coupling artefacts in BS-PS spectra; however, their multiplets in the carbohydrate region were homodecoupled by both PS approaches.

In addition to resolving multiplets into singlets to tackle overlapping issues, PS approaches can also be useful for confirming the presence of singlets in crowded regions. This is the case for choline, betaine, DMG, carnitine, glycine, *N* ^{1}-methyl-2-pyridone-5-carboxamide, 1-methylhistidine, 3-methyl-histidine and guanidoacetate signals located in the carbohydrate region. It is noteworthy that the confirmation of a metabolite assignment would be easier when the singlet in question is more intense than the rest of the overlapping signals, so the result could depend on the concentration in the sample. However, there is a possibility that singlets can be overshadowed by strong coupling artefacts from signals such as the singlet of DMG at δ 3.74 that overlaps with α-glucose and β-glucose (presence confirmed by *J*-Res spectra). Multiplicity-edited HSQC and HMBC methods are also useful to establish if the targeted singlet is a CH/CH_3 or CH_2, as implemented in the present study.

HOBS was able to homodecouple not only methyl groups, but also methylene and methine groups, even for signals that appear in a very compromised region such as the carbohydrate and aromatic regions: for example, PAG, pyroglutamate and hippurate in urine, and glucose, choline, lactate, proline and pyroglutamate in serum. In the case of the aromatic region, there are also metabolites whose homodecoupled signals can be seen using HOBS regardless of how compromised this region is in terms of signal overlap. This was exemplified for pseudouridine, 4-hydroxyhippurate, hippurate, paracetamol metabolites, and metabolites that are present at very low concentration such as trigonelline and 1-methylnicotinamide (Figure S12).

In summary, HOBS is effective, providing pure shifted signals when non-mutually coupled signals are excited by the selective pulse. For instance, the decoupled region, as depicted in both Figures 1 and 3, does not exhibit any mutually coupled signals. Instead, their coupled partners can be observed outside the selected region. However, Figure 4 shows how HOBS fails when mutually coupled signals are selected. This supports the value of applying HOBS for metabolite identification in complex mixtures such as urine and serum, due to its capacity of homodecoupling and sensitivity where no mutually coupled protons are present in the targeted region in question. However, the reader should be aware that HOBS

10991492, 0, Downloaded from https://analyticalsciencejournals.onlinelibrary.wiley.com/doi/10.1002/nbm.5060 by National Health And Medical Research Council, Wiley Online Library on [08/11/2023]. See the Terms and Conditions (https://onlinelibrary.wiley.com/terms-and-conditions) on Wiley Online Library for rules of use; OA articles are governed by the applicable Creative Commons License

may not always work, specifically for signals in the carbohydrate and aromatic regions. For instance, most of the signals of PAG were homodecoupled, with the exception of those in the aromatic region, and 4/4´and 2/2′ (Figure 4).

In the case of PSYCHE, the experiment is more tolerant to strong coupling, but has inherently lower sensitivity. Thus, this method is most useful for identifying metabolites present in high concentration, possibly in the millimolar range. This is the case for hippurate, PAG and *p*-CS in urine, and choline and glucose in serum. More details about the performance of these PS methods on specific metabolites can be observed in Tables 1 and 2. We acquired data in 10 ms chunks, but other widths such as 20 ms should be possible, for instance, in serum, a diluted sample where not much high dynamic range is present. We used a 15° flip angle as this was suggested in the manual to be a good general starting point, but did not optimize the angle specifically for this study.

The main differences between HOBS and PSYCHE in their performance, and the potential application to tackle the challenges of metabolite identification in urine and serum, are summarized in Figure 5.

Complex mixtures normally result in NMR spectra with some regions crowded with overlapping signals, where the concentration of the targeted metabolite(s) may be low and obscured by the resonances from other metabolites with similar chemical shifts that are present at higher concentrations. The combination of the high dynamic range and signal overlap may make it difficult to identify and confirm the presence of the targeted metabolite(s) in a given sample. PS experiments may be an option to reduce signal overlap in crowded regions/zones, which in turn makes these types of experiment a potential tool for metabolite identification. Accordingly, it is advisable to implement a multi-platform system for metabolite identification as recommended in the literature, in which PS experiments can also be included in the suite of 1D- and 2D-NMR experiments normally used for identification purposes.[28] As part of a holistic metabolic profiling framework, BS-PS can be useful for targeted or semi-targeted, and BB-PS for untargeted, studies. The utility of these pulse sequences will depend on the nature of the samples to be analysed and the type and parameter sets of the pulse sequence to be used. It is worth noting that these experiments are user friendly and do not require extensive spectrometer time (depending on the concentration of the metabolites relating to the signal/region of interest), and that both approaches are compatible with automation.

A couple of studies have been recently published using BB-PS for metabolic profiling to analyse extracts of plants and corals whose metabolites have a reasonable concentration range for applying this approach.[37,38] However, the use BB-PS for metabolic profiling of samples with metabolites that normally are at low concentration such as urine and serum is more of a challenge. Apart from the general utility of these pulse sequences, there are specific use cases where additional benefit is conferred. For example, BB-PS may be applied to urine samples from diabetic people to unveil and identify metabolites whose resonances are obscured by the resonances of glucose in the carbohydrate region. Moreover, new improvements in BS-PS regarding homodecoupling have been reported, which can also be useful to analyse complex mixtures.[16,17] The PS versions of 1D selective TOCSY also have the potential to aid metabolite identification in biosamples.[39,40] Concerning the water pre-saturation method utilized in this study, we did not optimize this and pragmatically used a method that is known to work well in automated high-throughput metabolic phenotyping studies. We note that since this manuscript was first submitted new approaches have been published to suppress the

Pure shift experiment	Sensitivity	Resolution	Time of experiment	Tolerance of strong couplings	Metabolite identification approach
HOBS	✓	✓	✓		Targeted
PSYCHE				✓	Untargeted
Challenge: urine[a]					
High dynamic range of compounds High variability of content and concentration (i.e., lack of homeostatic control) Presence of exogenous chemicals					
HOBS	Easier differentiation of phase 2 drug metabolites, dietary metabolic products, and endogenous metabolites at low concentration.				
PSYCHE	Easier differentiation of metabolites at good concentration that show strong coupled signals.				
Challenge: serum or plasma[a]					
Carbohydrate region dominated by sugars and amino acids. Overlap of lipoproteins and other macromolecules with low MW metabolites					
HOBS/HOBS-PROJECT	Easier differentiation of metabolites at low concentration. Filtering out of protein signals.				
PSYCHE	Perfect homodecoupling of carbohydrate signals to unveil overlapped resonances from other metabolites. Filtering out of protein signals.				
[a]Both pure shift experiments are able to confirm the presence of singlets in overlapped regions.					

FIGURE 5 Performance comparison of HOBS and PSYCHE for metabolite identification in two types of biofluid.

10991492, 0, Downloaded from https://analyticalsciencejournals.onlinelibrary.wiley.com/doi/10.1002/nbm.5060 by National Health And Medical Research Council, Wiley Online Library on [08/11/2023]. See the Terms and Conditions (https://onlinelibrary.wiley.com/terms-and-conditions) on Wiley Online Library for rules of use; OA articles are governed by the applicable Creative Commons License

water peak more effectively in PSYCHE spectra. These newly explored methods hold significant potential for enhancing future research efforts in analysing complex mixtures in aqueous media.[41] In addition to 1D-NMR PS experiments, there are 2D versions that can also be used for metabolite identification purposes; however, this would take substantially more experiment time.

4 | CONCLUSIONS

Considering all their benefits and limitations, PS experiments have a potential application for metabolite identification and might be included in the suite of 1D- and 2D-NMR pulse sequences routinely used to date for this purpose. BB-BS and BS-PS experiments are complementary, robust and easy to implement in biofluids. In addition, to save time during the NMR analysis, and for metabolite identification, PS experiments can be acquired in parallel with conventional 1D selective TOCSY and *J*-Res spectra. With the latter, it is possible to take advantage of the strong coupling artefacts for identification purposes, as they are part of the fingerprint of the metabolites that produce them. Thus, we have exemplified the application of PS experiments to metabolite identification in urine and serum and advocate further exploration of the use of these pulse sequences in the characterization of a broader range of biological fluids.

ACKNOWLEDGEMENTS

This article presents independent research funded by the UK National Institute for Health Research (NIHR) and the NIHR Imperial Biomedical Research Centre (BRC).

The authors would like to acknowledge the Imperial College NIHR-BRC Clinical Phenotyping Centre (CPC) for access to 800 MHz NMR facilities. We also thank the NMR Applications Support team at Bruker BioSpin for useful discussions regarding the NMR technology.

We also acknowledge the reviewers for their detailed and considered comments, specifically the detailed theoretical and practical expertise provided by Referee 3.

CONFLICT OF INTEREST STATEMENT

The authors declare that they have no conflict of interest.

ORCID

Jose Ivan Serrano-Contreras https://orcid.org/0000-0001-8669-7571
John C. Lindon https://orcid.org/0000-0002-0916-6360
Elaine Holmes https://orcid.org/0000-0002-0556-8389

REFERENCES

1. García-Pérez I, Posma JM, Gibson R, et al. Objective assessment of dietary patterns by use of metabolic phenotyping: a randomised, controlled, crossover trial. *Lancet Diabetes Endocrinol*. 2017;5(3):184-195. doi:10.1016/S2213-8587(16)30419-3
2. Holmes E, Loo RL, Stamler J, et al. Human metabolic phenotype diversity and its association with diet and blood pressure. *Nature*. 2008;453(7193):396-400. doi:10.1038/nature06882
3. Holmes E, Wilson ID, Nicholson JK. Metabolic phenotyping in health and disease. *Cell*. 2008;134(5):714-717. doi:10.1016/j.cell.2008.08.026
4. Nicholson JK, Holmes E, Kinross JM, Darzi AW, Takats Z, Lindon JC. Metabolic phenotyping in clinical and surgical environments. *Nature*. 2012;491(7424):384-392. doi:10.1038/nature11708
5. Ludwig C, Viant MR. Two-dimensional *J*-resolved NMR spectroscopy: review of a key methodology in the metabolomics toolbox. *Phytochem Anal*. 2010;21(1):22-32. doi:10.1002/pca.1186
6. Foxall PJ, Parkinson JA, Sadler IH, Lindon JC, Nicholson JK. Analysis of biological fluids using 600 MHz proton NMR spectroscopy: application of homonuclear two-dimensional *J*-resolved spectroscopy to urine and blood plasma for spectral simplification and assignment. *J Pharm Biomed Anal*. 1993;11(1):21-31. doi:10.1016/0731-7085(93)80145-Q
7. Holmes E, Foxall PJ, Spraul M, Farrant RD, Nicholson JK, Lindon JC. 750 MHz ^{1}H NMR spectroscopy characterisation of the complex metabolic pattern of urine from patients with inborn errors of metabolism: 2-hydroxyglutaric aciduria and maple syrup urine disease. *J Pharm Biomed Anal*. 1997;15(11):1647-1659. doi:10.1016/S0731-7085(97)00066-6
8. Moolenaar SH, van der Knaap MS, Engelke UF, et al. In vivo and in vitro NMR spectroscopy reveals a putative novel inborn error involving polyol metabolism. *NMR Biomed*. 2001;14(3):167-176. doi:10.1002/nbm.690
9. Fonville JM, Maher AD, Coen M, Holmes E, Lindon JC, Nicholson JK. Evaluation of full-resolution *J*-resolved ^{1}H NMR projections of biofluids for metabonomics information retrieval and biomarker identification. *Anal Chem*. 2010;82(5):1811-1821. doi:10.1021/ac902443k
10. Doskocz M, Marchewka Z, Jeż M, Passowicz-Muszyńska E, Długosz A. Preliminary study on *J*-resolved NMR method usability for toxic kidney's injury assessment. *Adv Clin Exp Med*. 2015;24(4):629-635. doi:10.17219/acem/33841
11. Dona AC, Jiménez B, Schafer H, et al. Precision high-throughput proton NMR spectroscopy of human urine, serum, and plasma for large-scale metabolic phenotyping. *Anal Chem*. 2014;86(19):9887-9894. doi:10.1021/ac5025039
12. Delaglio F, Walker GS, Farley KA, et al. Non-uniform sampling for all: more NMR spectral quality, less measurement time. *Am Pharm Rev*. 2017;20(4):339681.

10991492, 0, Downloaded from https://analyticalsciencejournals.onlinelibrary.wiley.com/doi/10.1002/nbm.5060 by National Health And Medical Research Council, Wiley Online Library on [08/11/2023]. See the Terms and Conditions (https://onlinelibrary.wiley.com/terms-and-conditions) on Wiley Online Library for rules of use; OA articles are governed by the applicable Creative Commons License

13. Foroozandeh M, Adams RW, Meharry NJ, Jeannerat D, Nilsson M, Morris GA. Ultrahigh-resolution NMR spectroscopy. *Angew Chem Int Ed Engl*. 2014;53(27):6990-6992. doi:10.1002/anie.201404111
14. Castañar L, Nolis P, Virgili A, Parella T. Full sensitivity and enhanced resolution in homodecoupled band-selective NMR experiments. *Chemistry*. 2013;19(51):17283-17286. doi:10.1002/chem.201303235
15. Zangger K. Pure shift NMR. *Prog Nucl Magn Reson Spectrosc*. 2015;86-87:1-20. doi:10.1016/j.pnmrs.2015.02.002
16. Ilgen J, Kaltschnee L, Thiele CM. perfectBASH: band-selective homonuclear decoupling in peptides and peptidomimetics. *Magn Reson Chem*. 2018;56(10):918-933. doi:10.1002/mrc.4757
17. Verma A, Bhattacharya S, Baishya B. Perfecting band selective homo-decoupling for decoupling two signals coupled within the same band. *RSC Adv*. 2018;8(36):19990-19999. doi:10.1039/C8RA01272E
18. Castañar L, Parella T. Broadband ^{1}H homodecoupled NMR experiments: recent developments, methods and applications. *Magn Reson Chem*. 2015;53(6):399-426. doi:10.1002/mrc.4238
19. Mycroft C, Nilsson M, Morris GA, Castañar L. Simultaneous broadband suppression of homonuclear and heteronuclear couplings in ^{1}H NMR spectroscopy. *ChemPhysChem*. 2022;23(24):e202200495. doi:10.1002/cphc.202200495
20. Castañar L, Nolis P, Virgili A, Parella T. Measurement of T_1/T_2 relaxation times in overlapped regions from homodecoupled ^{1}H singlet signals. *J Magn Reson*. 2014;244:30-35. doi:10.1016/j.jmr.2014.04.003
21. Bouatra S, Aziat F, Mandal R. The human urine metabolome. *PLoS ONE*. 2013;8(9):e73076. doi:10.1371/journal.pone.0073076
22. Bales JR, Sadler PJ, Nicholson JK, Timbrell JA. Urinary excretion of acetaminophen and its metabolites as studied by proton NMR spectroscopy. *Clin Chem*. 1984;30(10):1631-1636. doi:10.1093/clinchem/30.10.1631
23. Bales JR, Nicholson JK, Sadler PJ. Two-dimensional proton nuclear magnetic resonance "maps" of acetaminophen metabolites in human urine. *Clin Chem*. 1985;31(5):757-762. doi:10.1093/clinchem/31.5.757
24. Nicholson JK, Wilson ID. High resolution proton magnetic resonance spectroscopy of biological fluids. *Prog Nucl Magn Reson Spectrosc*. 1989;21(4/5):449-501. doi:10.1016/0079-6565(89)80008-1
25. Nicholson JK, Foxall PJ, Spraul M, Farrant RD, Lindon JC. 750 MHz ^{1}H and ^{1}H–^{13}C NMR spectroscopy of human blood plasma. *Anal Chem*. 1995;67(5):793-811. doi:10.1021/ac00101a004
26. Foroozandeh M, Morris GA, Nilsson M. PSYCHE pure shift NMR spectroscopy. *Angew Chem Weinheim Bergstr Ger*. 2018;24(53):13988-14000. doi:10.1002/chem.201800524
27. Cloarec O, Dumas ME, Craig A, et al. Statistical total correlation spectroscopy: an exploratory approach for latent biomarker identification from metabolic ^{1}H NMR data sets. *Anal Chem*. 2005;77(5):1282-1289. doi:10.1021/ac048630x
28. García-Pérez I, Posma JM, Serrano-Contreras JI, et al. Identifying unknown metabolites using NMR-based metabolic profiling techniques. *Nat Protoc*. 2020;15(8):2538-2567. doi:10.1038/s41596-020-0343-3
29. de Koning TJ, Snell K, Duran M, Berger R, Poll-The BT, Surtees R. L-serine in disease and development. *Biochem J*. 2003;371(3):653-661. doi:10.1042/bj20021785
30. Hashimoto K, Fukushima T, Shimizu E, et al. Decreased serum levels of D-serine in patients with schizophrenia: evidence in support of the *N*-methyl-D-aspartate receptor hypofunction hypothesis of schizophrenia. *Arch Gen Psychiatry*. 2003;60(6):572-576. doi:10.1001/archpsyc.60.6.572
31. de Koning TJ. Amino acid synthesis deficiencies. *J Inherit Metab Dis*. 2017;40(4):609-620. doi:10.1007/s10545-017-0063-1
32. Newman AC, Maddocks ODK. Serine and functional metabolites in cancer. *Trends Cell Biol*. 2017;27(9):645-657. doi:10.1016/j.tcb.2017.05.001
33. Wilson LA, Wilkinson K, Crews HM, Davies AM, Dick CS, Dumsday VL. Urinary monitoring of saccharin and acesulfame-K as biomarkers of exposure to these additives. *Food Addit Contam*. 1999;16(6):227-238. doi:10.1080/026520399283993
34. Maes P, Monakhova YB, Kuballa T, Reusch H, Lachenmeier DW. Qualitative and quantitative control of carbonated cola beverages using ^{1}H NMR spectroscopy. *J Agric Food Chem*. 2012;60(11):2778-2784. doi:10.1021/jf204777m
35. Ohtsuki T, Sato K, Abe Y, Sugimoto N, Akiyama H. Quantification of acesulfame potassium in processed foods by quantitative ^{1}H NMR. *Talanta*. 2015;131:712-718. doi:10.1016/j.talanta.2014.08.002
36. Engel J, Blanchet L, Engelke UF, Wevers RA, Buydens LM. Towards the disease biomarker in an individual patient using statistical health monitoring. *PLoS ONE*. 2014;9(4):e92452. doi:10.1371/journal.pone.0092452
37. López JM, Cabrera R, Maruenda H. Ultra-clean pure shift ^{1}H-NMR applied to metabolomics profiling. *Sci Rep*. 2019;9(1):6900. doi:10.1038/s41598-019-43374-5
38. Santacruz L, Hurtado DX, Doohan R, Thomas OP, Puyana M, Tello E. Metabolomic study of soft corals from the Colombian Caribbean: PSYCHE and ^{1}H-NMR comparative analysis. *Sci Rep*. 2020;10(1):5417. doi:10.1038/s41598-020-62413-0
39. Castañar L, Perez-Trujillo M, Nolis P, Monteagudo E, Virgili A, Parella T. Enantiodifferentiation through frequency-selective pure-shift ^{1}H nuclear magnetic resonance spectroscopy. *ChemPhysChem*. 2014;15(5):854-857. doi:10.1002/cphc.201301130
40. Dal Poggetto G, Castañar L, Morris GA, Nilsson M. A new tool for NMR analysis of complex systems: selective pure shift TOCSY. *RSC Adv*. 2016;6(102):100063-100066. doi:10.1039/C6RA22807K
41. Bertho G, Lordello L, Chen X, et al. Ultrahigh-resolution NMR with water signal suppression for a deeper understanding of the action of antimetabolic drugs on diffuse large B-cell lymphoma. *J Proteome Res*. 2022;21(4):1041-1051. doi:10.1021/acs.jproteome.1c00914

SUPPORTING INFORMATION

Additional supporting information can be found online in the Supporting Information section at the end of this article.

How to cite this article: Serrano-Contreras JI, Lindon JC, Frost G, Holmes E, Nicholson JK, Garcia-Perez I. Implementation of pure shift ^{1}H NMR in metabolic phenotyping for structural information recovery of biofluid metabolites with complex spin systems. *NMR in Biomedicine*. 2023;e5060. doi:10.1002/nbm.5060

10991492, 0, Downloaded from https://analyticalsciencejournals.onlinelibrary.wiley.com/doi/10.1002/nbm.5060 by National Health And Medical Research Council, Wiley Online Library on [08/11/2023]. See the Terms and Conditions (https://onlinelibrary.wiley.com/terms-and-conditions) on Wiley Online Library for rules of use; OA articles are governed by the applicable Creative Commons License